DYNAMIC TRANSITIONS AND TURING PATTERNS OF THE BRUSSELATOR MODEL

UMAR FARUK MUNTARI AND TAYLAN ŞENGÜL

ABSTRACT. The dynamic transitions of the Brusselator model has been recently analyzed in [1] and [2]. Our aim in this paper is to address the relation between the pattern formation and dynamic transition results left open in those papers. We consider the problem in the setting of a 2D rectangular box where an instability of the homogeneous steady state occurs due to the perturbations in the direction of several modes becoming critical simultaneously. Our main results are twofolds: (1) a rigorous characterization of the types and structure of the dynamic transitions of the model from basic homogeneous states and (2) the relation between the dynamic transitions and the pattern formations. We observe that the Brusselator model exhibits different transition types and patterns depending on the nonlinear interactions of the pattern of the critical modes.

1. Introduction

Dynamic transitions have been shown to occur in many branches of the nonlinear science [3]. Some recent examples include the thermohaline circulation [4], chemotatic systems [5], vegetation formation [6], gas dynamics [7] and quasi geostrophic flows [8, 9]. One of the jewels of the nonlinear science has been the Brusselator and related chemical reaction models which have received extensive interest [2, 10, 11]. In this paper, we identify and classify transitions of Turing patterns for the Brusselator model which was introduced initially in [12]. The model displays some important aspects of the dynamical systems theory such as multistability [13] and irreversibility [14]. Our main paradigm is the dynamic transition theory originally introduced in [3].

As an example of Belousov–Zhabotinsky reaction, the mechanism of the Brusselator model is based on autocatalytic, oscillating chemical reaction. An autocatlytic reaction is one in which a species acts to increase the rate of its producing reaction. In many autocatlytic systems, multiple steady-states and periodic orbits are usually seen [15]. The chemical reaction of the Brusselator model consists of four irreversible steps, given by

$$
\begin{aligned}
A &\overset{k_1}{\rightarrow} X \\
B + X &\overset{k_2}{\rightarrow} Y + D \\
2X + Y &\overset{k_3}{\rightarrow} 3X \\
X &\overset{k_4}{\rightarrow} E
\end{aligned} \tag{1}
$$

where X and Y are components which vary in time and space, A and B are constant components while D and E are products.

Turing patterns are natural patterns which arise spontaneously in a number of natural phenomena such as animal coatings, chemical reactions and patterns of sand dunes and vegetation patterns in ecology. The formations of these patterns are described by reaction-diffusion equations. A diffusion-driven instability also called the Turing instability occurs in a reaction-diffusion system when a homogeneous steady state is stable to small perturbation in the absence of diffusion but becomes unstable to small spatial perturbations when there is diffusion [16] . Mathematically, these equations possess a stable homogeneous equilibrium which will lose its stability as a control parameter exceeds some critical threshold. As this basic state loses stability, the system will move towards a new stable state, often displaying pattern structure which is known as Turing patterns.

In this article, we address the dynamic transition of Turing patterns of the Brusselator model by deriving a complete characterization of the transition from the homogeneous state. Our guiding principle is the dynamic transition theory of [3]. The key philosophy of dynamic transition theory is to search for the full set of transition states, giving a complete characterization of stability and transition. The set of transition states is a local attractor, representing the physical reality after the transition. As a general principle, dynamic transitions of all dissipative systems are classified into three categories: continuous (Type-I), catastrophic (Type-II), and random (Type-III) [17, 3]. In more mathematical intuitive terms, the types are respectively called continous, jump and mixed. In the Brusselator model, the signs of some nondimensional computable parameters determine the transition types.

There have been two recent papers [1, 2] which also dealt with the dynamic transitions of the Brusselator problem in different settings and with a different perspective. In [2], the emphasis is solely on the dynamic transitions and not on the pattern formations. More recently in [1] the problem is investigated in a one spatial variable setting. Although such simplifications are sometimes necessary to understand the basic mechanisms, to establish the relation between the pattern formations and dynamic transitions, at least two spatial variables are necessary which is the case studied in our paper. Thus the goal of the current paper is to address the shortcomings of these two papers.

The organization of this paper is as follows. Section 2 deals with the mathematical model, Section 3 focuses on the linear stability analysis and the principle of exchange of stabilities. The main theorems and the dynamic transitions of the model are addressed in Section 4, while the proofs of the theorems are discussed in Section 5 with the conclusion in Section 6.

2. The Model And Its Mathematical Setup

In this section, we present the mathematical representation of the Brusselator model together with the boundary conditions considered and then subsequently put it into an abstract functional setting. The classical Brusselator model of Prigogine and Lefever which in the nondimensionalized form reads

$$\begin{aligned} \partial_t u &= a - (b+1)u + u^2 v + d\Delta u \\ \partial_t v &= bu - u^2 v + \Delta v \end{aligned} \tag{2}$$

$a, b, d > 0$. We assume the Neuman boundary conditions on a 2D rectangular box.

$$\frac{\partial \mathbf{u}}{\partial n} = 0, \quad \mathbf{u} = (u, v) \qquad \text{on} \quad \partial\Omega, \quad \Omega = (0, L\pi) \times (0, \pi) \tag{3}$$

where n is the outer normal of the domain Ω.

The equations (2) admit the constant solution

$$(u_s, v_s) = (a, b/a)$$

The equations for the perturbations

$$\begin{pmatrix} u' \\ v' \end{pmatrix} = \begin{pmatrix} u \\ v \end{pmatrix} - \begin{pmatrix} u_s \\ v_s \end{pmatrix} \tag{4}$$

around this constant solution are as follows.

$$\partial_t \begin{pmatrix} u' \\ v' \end{pmatrix} = \begin{bmatrix} (b-1)+d\Delta & a^2 \\ -b & -a^2+\Delta \end{bmatrix} \begin{pmatrix} u' \\ v' \end{pmatrix} + \begin{bmatrix} \frac{b}{a}u'^2 + 2au'v' + u'^2v' \\ -\frac{b}{a}u'^2 - 2au'v' - u'^2v' \end{bmatrix} \tag{5}$$

We write (5) in the standard form by first defining the function spaces.

$$H = L^2(\Omega, \mathbb{R}^2) \tag{6}$$

$$H_1 = \left\{ \begin{pmatrix} u \\ v \end{pmatrix} \in H^2(\Omega, \mathbb{R}^2) : \frac{\partial u}{\partial n} = \frac{\partial v}{\partial n} = 0 \quad \text{on} \quad \partial\Omega \right\} \cap H, \tag{7}$$

$$H_{1/2} = \left\{ \begin{pmatrix} u \\ v \end{pmatrix} \in H^1(\Omega, \mathbb{R}^2) : \frac{\partial u}{\partial n} = \frac{\partial v}{\partial n} = 0 \quad \text{on} \quad \partial\Omega \right\} \cap H, \tag{8}$$

(9)

We also define the operators $L_b : H_1 \mapsto H$ and $G : H_{1/2} \mapsto H$ by

$$L_b \mathbf{u} = ((b-1)u + a^2 v + d\Delta u, -bu - a^2 v + \Delta v), \tag{10}$$

$$G(\mathbf{u}) = (\frac{b}{a}u^2 + 2auv + u^2 v, -\frac{b}{a}u^2 - 2auv - u^2 v) \tag{11}$$

Thus (5) can be written as

$$\frac{d\mathbf{u}}{dt} = L_b \mathbf{u} + G(\mathbf{u}) \tag{12}$$

3. Linear Stability Analysis

In this section, we analyze the linear stability of the basic steady state of the model. Then we formulate this analysis as principle of exchange of stabilities (PES), see Theorem 1.

For this purpose, we start with defining the index set

$$\mathcal{K} = (k_1, k_2) \in \mathbb{Z}^2_{\geq 0}, \tag{13}$$

the wavenumber

$$k^2 = \frac{k_1^2}{L^2} + k_2^2, \qquad k \in \mathcal{K},$$

and the **modes**

$$e_{k_1,k_2}(x, y) = \cos \frac{k_1}{L} x \cos k_2 y, \qquad (k_1, k_2) \in \mathcal{K}.$$

The mode is said to have a **rectangular pattern** if $k_1 \neq 0$, $k_2 \neq 0$ and a **roll pattern** if either $k_1 = 0$ or $k_2 = 0$. The particular case $k_1 = k_2 \neq 0$ of a rectangular pattern is called a **square pattern**.

For $k = (k_1, k_2) \in \mathcal{K}$, plugging the ansatz

$$\begin{bmatrix} u_k \\ v_k \end{bmatrix} e_{k_1,k_2}(x, y) \tag{14}$$

into the eigenvalue problem

$$L_b e_k = \beta_k e_k, \tag{15}$$

yields the eigenvalue relation

$$\beta_k \begin{bmatrix} u_k \\ v_k \end{bmatrix} = A \begin{bmatrix} u_k \\ v_k \end{bmatrix} - k^2 D \begin{bmatrix} u_k \\ v_k \end{bmatrix} \tag{16}$$

where the operators A and D stand for

$$A = \begin{bmatrix} b-1 & a^2 \\ -b & -a^2 \end{bmatrix}, \qquad D = \begin{bmatrix} d & 0 \\ 0 & 1 \end{bmatrix}$$

We can easily show that the eigenvectors are given by

$$\begin{bmatrix} u_k \\ v_k \end{bmatrix} = \begin{bmatrix} 1 \\ \frac{-b}{\beta_k + a^2 + k^2} \end{bmatrix} \tag{17}$$

and the eigenvalues satisfy

$$\det(\beta_k I - (A - k^2 D)) = \beta_k^2 - \tau_k \beta_k + \Delta_k = 0 \tag{18}$$

where

$$\tau_k = \operatorname{tr}(A - k^2 D) = b - 1 - a^2 - (d+1)k^2 \tag{19}$$

and

$$\Delta_k = \det(A - k^2 D) = a^2 + (a^2 d + 1 - b)k^2 + dk^4 \tag{20}$$

Hence the eigenvalues are

$$\beta_k = \frac{\tau_k \pm \sqrt{\tau_k^2 - 4\Delta_k}}{2} \tag{21}$$

Turing instability is defined as the stability of the equilibrium without diffusion, i.e. $k = 0$ case, while instability with diffusion for some $k \neq 0$. This was the original idea of Turing which was a novel one since diffusion is often a stabilizing mechanism.

Since $\Delta_0 = \det(A) = a^2 > 0$, the stability of the equilibrium without diffusion only requires

$$\tau_0 = \operatorname{tr}(A) = b - 1 - a^2 < 0 \tag{22}$$

From (18), the instability in the presence of diffusion means that for some $k \neq 0$, exactly one of the following conditions (23), (24) holds:

$$\Delta_k < 0 \tag{23}$$

or

$$\Delta_k > 0 \qquad \text{and} \qquad \tau_k > 0. \tag{24}$$

Since $\tau_k \leq \tau_0$, $\tau_0 < 0$ implies that $\tau_k < 0$ for any k, (22) and (24) are incompatible. Thus for the Turing instability, one requires the following two conditions to hold.

$$\tau_0 < 0, \text{ and } \Delta_k < 0 \text{ for some } k \in \mathcal{K}. \tag{25}$$

The **critical Turing wave number** $k_T \in \mathcal{K}$ is determined as

$$k_T = \operatorname{argmin}_{k \in \mathcal{K}} \Delta_k. \tag{26}$$

To obtain k_T, we first consider the problem

$$0 = \frac{d}{dk^2}\Delta_k = \frac{d}{dk^2}\det(A - k^2 D) = \operatorname{tr}(D^{-1}A - k^2 I), \qquad k^2 \in \mathbb{R}^+. \tag{27}$$

whose solution is

$$\tilde{k}^2 = \frac{1}{2}\operatorname{tr}(D^{-1}A) = \frac{b - 1 - a^2 d}{2d}. \tag{28}$$

The **critical transition number** b_T is now determined by solving b from the relation

$$0 = \Delta_{\tilde{k}} = -\frac{(b-1)^2 - 2a^2(1+b) + a^4 d^2}{4d}$$

and is obtained as

$$b = (a\sqrt{d} \pm 1)^2.$$

However, only $b = (a\sqrt{d} + 1)^2$ in (28) gives a positive $\tilde{k}^2$. Thus we define

$$b_T = (a\sqrt{d} + 1)^2$$

Suppose that for $k_1, k_2 \in K$,

$$k_1^2 \le \tilde{k}^2 \mid_{b=b_T} = \frac{a}{\sqrt{d}} \le k_2^2.$$

Then we define $k_T \in \mathcal{K}$ as

$$k_T^2 = \operatorname{argmin}_{k \in \{k_1, k_2\}} \Delta_k. \tag{29}$$

Since

$$\frac{d\Delta_k}{db} = -k^2 < 0$$

the following transversality condition is satisfied

$$\Delta_{k_T} \begin{cases} > 0 & b < b_T \\ = 0 & b = b_T \\ < 0 & b > b_T \end{cases} \tag{30}$$

which ensures the PES condition given in Theorem 1. Let us define

$$b_H = a^2 + 1$$

so that the condition $\tau_0 < 0$ is equivalent to the condition $b < b_H$. Hence Turing instability is possible if $b_T < b_H$ which is equivalent to the condition

$$\sqrt{d} < \frac{\sqrt{1+a^2} - 1}{a}$$

In this case, solving $\beta_k = 0$ which is equivalent to $\Delta_k = 0$ gives neutral stability curves

$$b = \frac{(a^2 + k^2)(1 + dk^2)}{k^2}.$$

This is illustrated in Figure 1.

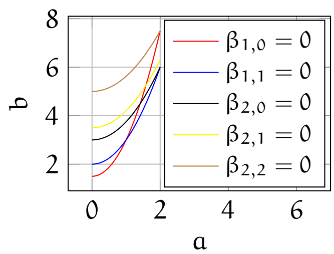

FIGURE 1. The neutral stability curves above which the eigenvalue with given wave number $k \in \mathcal{K}$ is unstable in the $a-b$ plane. Here $d = 0.5$, $L = 1$.

As a result of the above discussion, we can write the following theorem which is known as the Principle of Exchange of Stabilities (PES).

Theorem 1. *Suppose that $\sqrt{d} < \frac{\sqrt{1+a^2}-1}{a}$. Then the basic steady state is stable without diffusion, that is when $d = 0$. In the presence of diffusion, $d \neq 0$, the basic steady state loses its stability as b exceeds $b_T = (a\sqrt{d}+1)^2$. In particular the linear operator has finitely many real eigenvalues with wavenumber k_T as defined in (29) which cross the imaginary axis as b exceeds b_T while the rest of its spectrum lies in the negative complex half plane.*

Another possibility of transition is the Hopf transition which occurs when $\operatorname{tr}(A) = 0$ while $\det(A) > 0$. In this case a pair of complex eigenvalues cross the imaginary axis. It can be shown that Hopf bifurcation is possible when $\sqrt{d} > \frac{\sqrt{1+a^2}-1}{a}$, see Figure 2. However we will not discuss this case in this study.

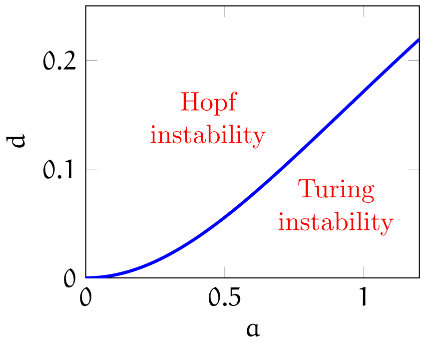

FIGURE 2. Hopf vs Turing instability in the parameter space.

4. MAIN TRANSITION THEOREMS

As illustrated in Figure 1, depending on the parameters of the system, the first critical mode(s) can have either a roll pattern or a rectangular pattern. We recall that the first critical modes have roll pattern if its wavenumber is $(k, 0)$, $k \neq 0$ or have rectangular pattern if its wavenumber is (j, k), $j \neq 0$, $k \neq 0$. Also depending on the parameters, several of these modes may become unstable simultaneously. In this paper, our aim is to identify the transitions associated with these critical crossings.

4.1. Single rectangular mode transition. The first case we consider is a single critical mode with a rectangular spatial pattern with wavenumber $k_T = (j_1, j_2)$, $j_1 \neq 0$, $j_2 \neq 0$. Then near the onset of transition, we find that Landau equation for the amplitude of this critical mode is as follows.

$$\frac{dx}{dt} = \beta_{j_1,j_2} x_1 + A x_1^3 + o(3) \tag{31}$$

$$A = \frac{c}{16}\left(4M_{00} + 2M_{20} + 2M_{02} + M_{22}\right), \quad c > 0. \tag{32}$$

and x is the time dependent amplitude of the first critical mode, β_{j_1,j_2} is the critical eigenvalue. Moreover, the other terms are defined as follows.

$$c = \frac{(a^2 + k_T^2 + b_T)(a^2 + k_T^2)}{((a^2 + k_T^2)^2 + b_T^2)} \tag{33}$$

and the other parameter as also given by the following,

$$\begin{aligned} M_k &= \frac{(\phi_1\phi_2 + \phi_1\phi_3\nu_k)V_k}{\beta_k}, \\ V_k &= \frac{\nu_k - 1}{\nu_k^2 + 1}, \quad \nu_k = \frac{-b_T}{\beta_k + a^2 + k^2}, \qquad k \in \mathcal{K}. \end{aligned} \tag{34}$$

$$\begin{aligned} \phi_1 &= \frac{(k_T^2 - a^2)b_T}{a(a^2 + k_T^2)}, \\ \phi_2 &= \frac{2k_T^2 b_T}{a(a^2 + k_T^2)}, \\ \phi_3 &= 2a. \end{aligned} \tag{35}$$

Theorem 2. *Suppose that the conditions of Theorem 1 holds and the first critical mode has a rectangular pattern with wavenumber $k_T = (j_1, j_2)$, $j_1 \neq 0$ and $j_2 \neq 0$. Then the system (2) has a transition at $b = b_T$ which depends on the number A defined in (31) and a special case of which is as shown in Figure 3. The following conclusions also hold true:*

(1) *If $A > 0$ system (2) has a **jump transition** accompanied by **subcritical pitchfork bifurcation** at $b = b_T$. In particular, there are no bifurcated steady states on $b > b_T$ and there are exactly two bifurcated solutions v_+^b and v_-^b which are saddles when $b < b_T$. Also, for $b < b_T$, the stable manifolds of these bifurcated steady states divide the phase plane H into three disjoint open sets U_+^b, U_0^b and U_-^b such that $v = 0 \in U_0^b$ is an attractor, and the orbits in $U_\pm^b$ are far from $v = 0$.*

(2) *If $A < 0$ system (2) has a **continuous transition** accompanied by **supercritical pitchfork bifurcation** at $b = b_T$. In particular, there are no bifurcated steady states on $b < b_T$ and there are exactly two bifurcated solutions u_+^b and u_-^b which are attractors when $b > b_T$. Also there is a neighborhood $O \subseteq H$ of $u = 0$, such that the stable manifold of $u = 0$ divides O into two disjoint open sets U_+^b and U_-^b such that $u_+^b \in U_+^b$, $u_-^b \in U_-^b$ and $u_\pm$ attracts $U_\pm^b$.*

(3) *The bifurcated steady state solutions are defined only for $\beta_{j_1,j_2} A < 0$ and are given by*

$$v_\pm^b = \pm\sqrt{\frac{-\beta_{j_1,j_2}}{A}} \cos\left(\frac{j_1 x}{L}\right) \cos j_2 y + o(\sqrt{-\beta_{j_1,j_2}}) \quad \textit{or} \tag{36}$$

$$u_\pm^b = \pm\sqrt{\frac{-\beta_{j_1,j_2}}{A}} \cos\left(\frac{j_1 x}{L}\right) \cos j_2 y + o(\sqrt{-\beta_{j_1,j_2}}) \tag{37}$$

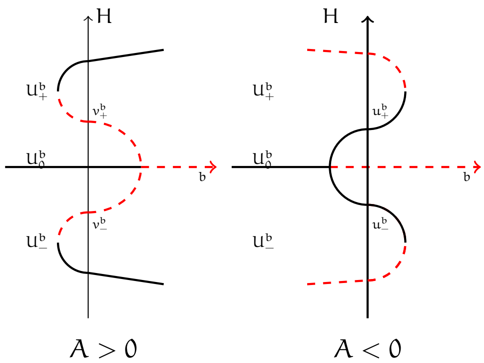

FIGURE 3. The bifurcation diagram for the Turing instability when the first critical wavenumber is $k_T = (1, 1)$. The bifurcation is subcritical pitchfork when $A > 0$ and supercritical pitchfork when $A < 0$ where A is given by (31).

Figure 3 in essence summarizes Theorem 2 and displays the types of bifurcation that occurs depending on the sign of A.

To better understand the dependence of the transition number A in (32) on the system parameters, we consider a specific case where the domain is a square, the aspect ratio $L = 1$ and the first critical mode has patterns with $j_1 = j_2 = 1$. In this specific case, there exist pairs $(a, d) \in \Omega_1$ on the $a - d$ plane where $A > 0$ and pairs $(a, d) \in \Omega_2$ where $A < 0$, see Figure 4.

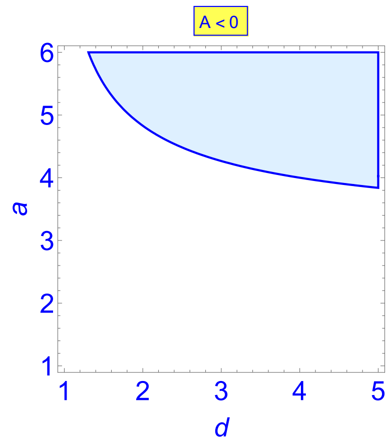

FIGURE 4. The transition type for single rectangular mode transition in the $a-d$ parameter space for the special case $j_1 = j_2 = 1$ and aspect ratio $L = 1$. The unshaded region represents **jump transition** while the shaded region represents **continuous transition**.

4.2. **Single roll mode transition.** Next, we turn to the transition scenario of a single critical roll pattern mode with wavenumber

$$k_T = (j_1, 0), \quad j_1 \neq 0$$

. In this case, our analysis shows that the Ginzburg Landau equation for this single mode is given by

$$\frac{dx_1}{dt} = \beta_{j_1,0} x_1 + B x_1^3 + O(4) \tag{38}$$

where x_1 is the time dependent amplitude of the first critical mode and $\beta_{j_1,0}$ is the critical eigenvalue. The coefficient of the cubic term is as follows.

$$B = \frac{c}{4}\left(2M_{00} + M_{20}\right) \tag{39}$$

The transition theorem in this case is similar to that of Theorem 2 and the bifurcation diagram for the transition number B is similar to that of A. The system (2) exhibits **continuous transition** when $B < 0$ and **jump transition** when $B > 0$ see Figure 5 .

The bifurcated steady state solutions defined only when $\beta_{j_1,0} B < 0$ can be expressed as

$$w_{\pm}^{b} = \pm\sqrt{\frac{-\beta_{j_1,0}}{B}} \cos\left(\frac{j_1 x}{L}\right) + o(\sqrt{-\beta_{j_1,0}}) \tag{40}$$

4.3. **Double roll mode transition.** We consider the critical crossing of two roll modes with common wavenumber

$$k_T^2 = k_{j_1,0}^2 = k_{0,j_2}^2$$

and the critical length scale

$$L = \frac{j_1}{j_2}$$

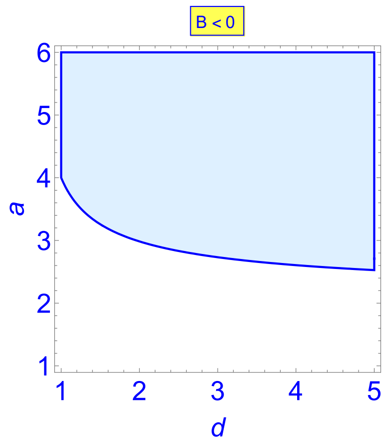

FIGURE 5. The transition type for single roll mode in the parameter space $a - d$ for the special case $j_1 = 1$ and aspect ratio $L = 1$. The unshaded region represents **jump transition** while the shaded region represents **continuous transition**.

Then near the onset of transition, we find the Landau equations for the amplitudes of these modes as

$$\begin{aligned} \frac{dx_1}{dt} &= \beta_{j_1,0}x_1 + D_1x_1x_2^2 + D_2x_1^3 + o(3) \\ \frac{dx_2}{dt} &= \beta_{0,j_2}x_2 + D_1x_1^2x_2 + D_3x_2^3 + o(3) \end{aligned} \tag{41}$$

where x_1 and x_2 are the time dependent amplitudes of the critical modes and $\beta_{j_1,0}$, β_{0,j_2} are the critical eigenvalues.

$$\begin{aligned} D_1 &= \frac{c}{2}\left(M_{00} + 2M_{11}\right) \\ D_2 &= \frac{c}{4}\left(2M_{00} + M_{20}\right) \\ D_3 &= \frac{c}{4}\left(2M_{00} + M_{02}\right) \end{aligned} \tag{42}$$

Thus

$$D_2 = B.$$

and in the case $j_1 = j_2, D_2 = D_3$. Figure 6 shows plots of D_1, D_2 in the $a - d$ parameter space.

To describe the bifurcated solutions, as in [18], first we assume the following non-degeneracy conditions.

$$D_2 \neq 0, \quad D_1 + D_2 \neq 0, \quad \beta_{j_1,0}D_2 < 0, \quad \beta_{j_1,0}(D_1 + D_2) < 0. \tag{43}$$

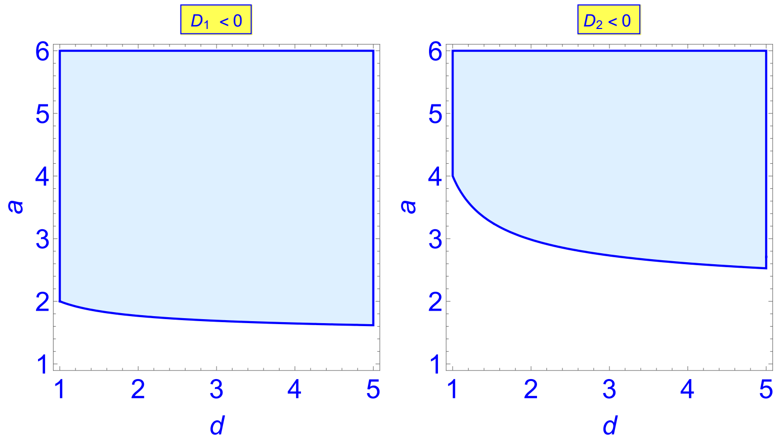

FIGURE 6. Plots of D_1(left) and D_2(right) in the $a-d$ parameter space for the case $j_1 = j_2 = 1$ and hence $D_2 = D_3$. The shaded regions respectively show where D_1 and D_2 are negative.

$$\begin{aligned}
\varphi_i &= (-1)^i \sqrt{\frac{\beta_{j_1,0}}{-D_2}} \cos\left(\frac{j_1 x}{L}\right) \begin{pmatrix} 1 \\ \nu_{j_1,0} \end{pmatrix}, && i = 1,2 \\
\varphi_i &= (-1)^i \sqrt{\frac{\beta_{0,j_2}}{-D_2}} \cos j_2 y \begin{pmatrix} 1 \\ \nu_{0.j_2} \end{pmatrix}, && i = 3,4 \\
\varphi_i &= c_i \cos\left(\frac{j_1 x}{L}\right) \begin{pmatrix} 1 \\ \nu_{j_1,0} \end{pmatrix} + d_i \cos j_2 y \begin{pmatrix} 1 \\ \nu_{0,j_2} \end{pmatrix}, && i = 5,6,7,8
\end{aligned}$$

where

$$c_5 = c_6 = -c_7 = -c_8 = \sqrt{\frac{\beta_{j_1,0}}{-(D_1 + D_2)}}$$

$$d_5 = -d_6 = d_7 = -d_8 = \sqrt{\frac{\beta_{j_1,0}}{-(D_1 + D_2)}}$$

Thus $\varphi_1, \varphi_2, \varphi_3$ and φ_4 are the roll modes with critical wave number $k_T^2 = 1$ while $\varphi_5, ..., \varphi_8$ are mixed modes which are the superposition of the roll modes.

Theorem 3. *Assume the aspect ratio is $L = \frac{j_1}{j_2}$ and the first two critical modes have wavenumbers $k_T = (j_1, 0)$ and $k_T = (0, j_2)$ such that $j_1 = j_2$. Then the system undergoes a first transition as b exceeds b_T. Moreover, under the assumption (43), the system has a continuous (respectively jump) transition accompanied by a bifurcated attractor (respectively repeller) Σ_b on $b > b_T$ (respectively on $b < b_T$) depending on D_1, D_2. Σ_b is homeomorphic to the circle S^1 and contains the steady states together with connecting heteroclinic orbits.*

We let $N(\Sigma_b)$ denote the number of steady states on Σ_b, S denotes stable steady states, and U denote the unstable steady states on Σ_b. We have the following characterization of Σ_b which is also given in Figure 7 and Figure 8.

(i) *If $D_1 < D_2 < 0$ then Σ_b is an attractor such that $N(\Sigma_b) = 8$, $S = \{\varphi_i | i = 1, 2, 3, 4\}$, $U = \{\varphi_i | i = 5, 6, 7, 8\}$.*

(ii) *If $D_2 < D_1 < 0$ or $D_2 < 0 < D_1$ $D_1 + D_2 < 0$ then Σ_b is an attractor such that $N(\Sigma_b) = 8$, $S = \{\varphi_i | i = 5, 6, 7, 8\}$, $U = \{\varphi_i | i = 1, 2, 3, 4\}$.*

(iii) *If* $D_2 < 0 < D_1$, $D_1 + D_2 > 0$, *then* Σ_b *is a repeller such that* $N(\Sigma_b) = 4$, $U = \{\varphi_i | i = 1, 2, 3, 4\}$.

(iv) *If* $D_2 > D_1 > 0$, *then* Σ_b *is a repeller such that* $N(\Sigma_b) = 4$, $U = \{\varphi_i | i = 5, 6, 7, 8\}$.

(v) *If* $D_2 > 0 > D_1$, $D_1 + D_2 < 0$, *then* Σ_b *is a repeller such that* $N(\Sigma_b) = 4$, $U = \{\varphi_i | i = 5, 6, 7, 8\}$.

(vi) $D_2 > 0 > D_1$ *or* $D_2 > D_1 > 0$, $D_1 + D_2 > 0$, *then* Σ_b *is an attractor such that* $N(\Sigma_b) = 4$, $S = \{\varphi_i | i = 5, 6, 7, 8\}$.

From Theorem 3, the structure of the attractor depends on the signs of D_1, D_2. Figure 7 and Figure 8 show the possible transitions from Theorem 3. Table 1 provides the summary of the steady states, condition of existence and stability.

Steady State	Existence	Stability
φ_1, φ_2	$\beta_{j_1,0} D_2 < 0$	$D_1 < D_2 < 0$
φ_3, φ_4	$\beta_{0,j_2} D_2 < 0$	$D_1 < D_2 < 0$
$\varphi_5, \varphi_6, \varphi_7, \varphi_8$	$\beta_{j_1,0}(D_1 + D_2) < 0$, $\beta_{0,j_2}(D_1 + D_2) < 0$	$D_2 < D_1 < 0$

TABLE 1. Existence and stability conditions for steady states of the double roll mode transitions.

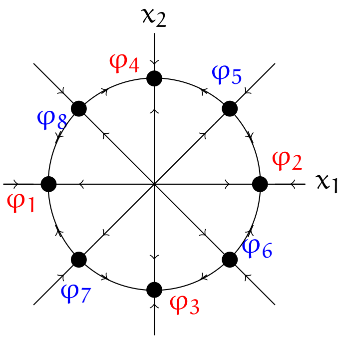

FIGURE 7. $D_1 < D_2 < 0$

.

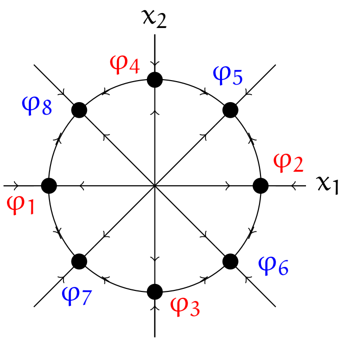

FIGURE 8. $D_2 < D_1 < 0$ (or $D_2 < 0 < D_1$), $D_1 + D_2 < 0$

.

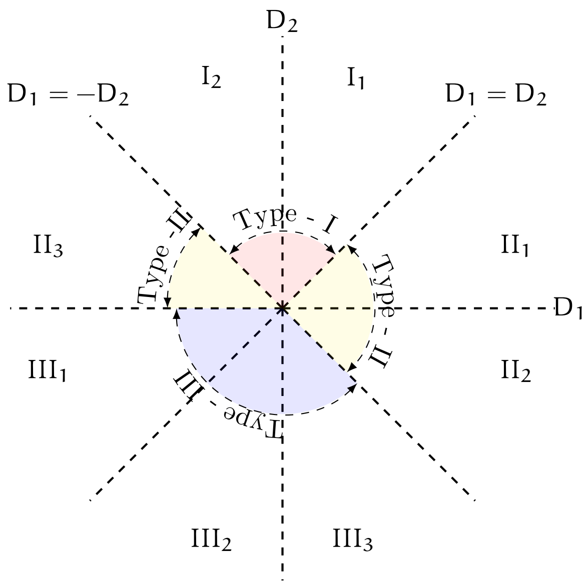

FIGURE 9. Classification of transition types for the double roll mode: Continuous Type-I, Jump Type-II, Mixed Type III. See Figure 7 and Figure 8 for the topological structures of III_1, III_2 and III_3.

4.4. **A roll and a rectangular mode transition.** Now we consider the interactions of a roll mode with a square mode. To understand the formation of hexagonal patterns, we let the critical wave number be as follows

$$k_T^2 = k_{2j_1,0}^2 = k_{j_1,j_2}^2 \tag{44}$$

Such that the critical length scale,

$$L = \frac{j_1\sqrt{3}}{j_2}.$$

Moreover, we assume that one of the first two critical modes has a square pattern and the other has a roll pattern.

Under the above assumptions and near $b = b_T$, we let $\beta_{j_1,0} = \beta_{j_1,j_2} = \beta$, then we obtain that the dynamics of the system is dictated by the following ODE system

$$\begin{aligned} \frac{dx_1}{dt} &= \beta x_1 + A_1 x_1 x_2 \quad + x_1(A_2 x_1^2 + A_3 x_2^2) + O(4) \\ \frac{dx_2}{dt} &= \beta x_2 + B_1 x_1^2 \quad\quad + x_2(B_2 x_1^2 + B_3 x_2^2) + O(4) \end{aligned} \tag{45}$$

$$\begin{aligned} &A_1 = c\phi_1, \quad A_2 = \frac{c}{16}\Big(M_{22} + 4M_{00}\Big), \quad A_3 = \frac{c}{2}\Big(M_{00} + 2M_{31}\Big) \\ &B_1 = \frac{c\phi_1}{4}, \quad B_2 = \frac{c}{2}\Big(M_{00} + 2M_{31}\Big), \quad B_3 = \frac{c}{4}\Big(2M_{00} + M_{40}\Big) \end{aligned} \tag{46}$$

Thus from (46), we observe that $A_1 = 4B_1$ and $A_3 = B_2$.

For the analysis of (45), we assume the following non-degeneracy conditions.

$$B_3 \neq 0, \qquad A_1 B_1 \neq 0. \tag{47}$$

To discuss the bifurcated steady states, we define the following pure and mixed solutions as follows.

$$\varphi_i = (-1)^i \sqrt{-\frac{\beta}{B_3}} \cos(j_2 y) \begin{pmatrix} 1 \\ \nu_{0,j_2} \end{pmatrix}, \qquad i = 1,2$$

$$\varphi_i = (-1)^i \frac{1}{\sqrt{A_1 B_1}} \beta \cos\left(\frac{j_1 x}{L}\right) \cos(j_2 y) \begin{pmatrix} 1 \\ \nu_{j_1,j_2} \end{pmatrix} - \frac{1}{A_1} \beta \cos(j_2 y) \begin{pmatrix} 1 \\ \nu_{0,j_2} \end{pmatrix}, \quad i = 3,4$$

Thus φ_1, φ_2 are the pure modes modes while φ_3, φ_4 are the mixed modes. In what follows, we provide the key aspects of the transition theory of system (45). We note that the transition of the system depends on the coefficients A_1, B_2 and B_3 while the rest of the coefficients only play quantitative role. For full details of the theorem, the stability and existence of the steady states as well as the related transition diagrams and detailed analysis, we refer the interested reader to [17] and the proofs there in.

Theorem 4. ***For*** $A_1 B_1 > 0$,

(i) *If* $B_3 < 0$, *then the system* (45) *undergoes a random (Type - III) transition near* $b = b_T$.

(ii) *If* $B_3 > 0$, *then the system* (45) *undergoes a catastrophic (Type - II) transition at* $b = b_T$.

For $A_1 B_1 < 0$,

(i) *If* $B_3 < 0$, *then the system* (45) *undergoes a continuous (Type - I) transition near* $b = b_T$.

(ii) *If* $B_3 > 0$, *then the system* (45) *undergoes a catastrophic (Type - II) transition at* $b = b_T$.

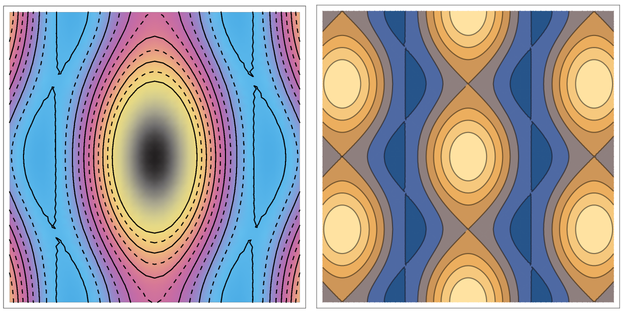

FIGURE 10. Density Plot (left), Contour Plot (right) of Sample Mixed Mode Patterns, $\cos\left(\frac{x}{\sqrt{3}}\right)\cos(y) + \cos\left(\frac{2x}{\sqrt{3}}\right)$ as applied to Theorem 4.

5. PROOFS

In this section, we present the proofs of our main theorems using the center manifold reduction criteria to establish amplitude equations for various modes of transitions.

5.1. CENTER MANIFOLD REDUCTION.

We write our solution as follows

$$\begin{pmatrix} u \\ v \end{pmatrix} = \sum_{k=1}^{r} x_k \begin{pmatrix} u_k \\ v_k \end{pmatrix} e_{k_1,k_2} + \begin{pmatrix} \Phi_u \\ \Phi_v \end{pmatrix} \tag{48}$$

where r is the number of critical modes while Φ_u and Φ_v are the u and v components of the center manifold function.

$$e_{k_1,k_2} = \cos\frac{k_1}{L}x\cos k_2 y$$

We adopt the following notations for simplicity.

$$e_{mn} = \cos(\frac{mj_1x}{L})\cos(nj_2y) \quad m,n\in\mathbb{Z}^+\cup\{0\}$$

$$f_{mn} = e_{mn}$$

For example $f_{20} = e_{2j_10}$, $f_{11} = e_{j_1j_2}$.

5.1.1. *Single rectangular mode transition.* We consider a single critical mode with rectangular pattern

$$f_{11} = e_{j_1j_2} = \cos\frac{j_1}{L}x\cos j_2 y$$

$$\begin{pmatrix} u \\ v \end{pmatrix} = x(t)\begin{pmatrix} u_{j_1,j_2} \\ v_{j_1,j_2} \end{pmatrix} f_{11} + \begin{pmatrix} \Phi_u \\ \Phi_v \end{pmatrix} \tag{49}$$

where $\begin{pmatrix} u_{j_1,j_2} \\ v_{j_1,j_2} \end{pmatrix} f_{11}$ is the critical eigenvector and

$$\begin{aligned} \begin{pmatrix} \Phi_u \\ \Phi_v \end{pmatrix} = \Phi_{00}\begin{pmatrix} u_{0,0} \\ v_{0,0} \end{pmatrix} f_{00} + \Phi_{20}\begin{pmatrix} u_{2j_1,0} \\ v_{2j_1,0} \end{pmatrix} f_{20} \\ + \Phi_{02}\begin{pmatrix} u_{0,2j_2} \\ v_{0,2j_2} \end{pmatrix} f_{02} + \Phi_{22}\begin{pmatrix} u_{2j_1,2j_2} \\ v_{2j_1,2j_2} \end{pmatrix} f_{22} \end{aligned} \tag{50}$$

where

$$\begin{aligned} \Phi_{00} &= q_{00}x^2 \\ \Phi_{20} &= q_{20}x^2 \\ \Phi_{02} &= q_{02}x^2 \\ \Phi_{22} &= q_{22}x^2 \end{aligned} \tag{51}$$

By substituting the central part of (49) into (12) we have

$$f_{11}\begin{pmatrix} u_{j_1,j_2} \\ v_{j_1,j_2} \end{pmatrix}\frac{dx(t)}{dt} = x\begin{pmatrix} u_{j_1,j_2} \\ v_{j_1,j_2} \end{pmatrix}\beta_{j_1,j_2}f_{11} + \begin{pmatrix} g_1(u,v) \\ g_2(u,v) \end{pmatrix} \tag{52}$$

where

$$G(\mathbf{u}) = \begin{pmatrix} g_1(u,v) \\ g_2(u,v) \end{pmatrix}$$

We take the inner product of (52) with $\begin{pmatrix} u_{j_1,j_2} \\ v_{j_1,j_2} \end{pmatrix} f_{11}$ and obtain the following equation

$$\begin{aligned} \frac{dx(t)}{dt} &= \beta_{j_1,j_2}x(t) + \left(\frac{1-v_{j_1,j_2}}{1+v_{j_1,j_2}^2}\right)\frac{\langle g_1(u,v), f_{11}\rangle}{\langle f_{11}, f_{11}\rangle} \\ \frac{dx(t)}{dt} &= \beta_{j_1,j_2}x(t) + c\frac{\langle g_1(u,v), f_{11}\rangle}{\langle f_{11}, f_{11}\rangle} \end{aligned} \tag{53}$$

where c is a positive constant given by

$$c = \left(\frac{1-v_{j_1,j_2}}{1+v_{j_1,j_2}^2}\right) = \frac{(a^2+k_T^2+b_T)(a^2+k_T^2)}{((a^2+k_T^2)^2+b_T^2)}$$

$$
\begin{aligned}
g_1(u,v) &= \frac{b}{a}u^2 + 2auv + \text{h.o.t} \\
&= \left(\frac{b}{a} + 2av_{j_1,j_2}\right) x_1^2 f_{11}^2 + \left(2\frac{b}{a} + 2av_{j_1,j_2}\right) x_1 f_{11}\Phi_u + 2ax_1 f_{11}\Phi_v \\
&= \phi_1 x_1^2 f_{11}^2 + \phi_2 x_1 f_{11}\Phi_u + \phi_3 x_1 f_{11}\Phi_v
\end{aligned} \tag{54}
$$

$\phi_i, i = 1,2,3$ are as defined in (35) and we have made the substitution $u_{11} = 1$.

We define G_{21} as the quadratic part of $g_1(u,v)$ as follows

$$
G_{21} = \phi_1 x_1^2 f_{11}^2 \tag{55}
$$

Also

$$
\langle f_1, f_2, f_3\rangle = \int_\Omega (f_1 f_2 f_3) d\mu, \quad \langle f_1, f_2\rangle = \int_\Omega (f_1 f_2) d\mu
$$

$$
\langle g_1, f_{11}\rangle = \phi_1 x_1^2 \langle f_{11}^2, f_{11}\rangle + \phi_2 x_1 \langle f_{11}\Phi_u, f_{11}\rangle + \phi_3 x_1 \langle f_{11}\Phi_v, f_{11}\rangle \tag{56}
$$

The inner products in (56) are as follows.

(57)

$$
\begin{aligned}
\langle f_{11}\Phi_u, f_{11}\rangle &= \Phi_{00}\langle f_{11}f_{00}, f_{11}\rangle + \Phi_{20}\langle f_{11}f_{20}, f_{11}\rangle + \Phi_{02}\langle f_{11}f_{02}, f_{11}\rangle \\
&\quad + \Phi_{22}\langle f_{11}f_{22}, f_{11}\rangle \\
&= \frac{L\pi^2}{16}(4\Phi_{0,0} + 2\Phi_{20} + 2\Phi_{02} + \Phi_{22}) \\
\langle f_{11}\Phi_v, f_{11}\rangle &= \Phi_{00}v_{0,0}\langle f_{11}f_{00}, f_{11}\rangle \Phi_{20}v_{2j_1,0}\langle f_{11}f_{20}, f_{11}\rangle + \Phi_{02}v_{0,2j_2}\langle f_{11}f_{02}, f_{11}\rangle \\
&\quad + \Phi_{22}v_{2j_1,2j_2}\langle f_{11}f_{22}, f_{11}\rangle \\
&= \frac{L\pi^2}{16}(4\Phi_{0,0}v_{0,0} + 2\Phi_{20}v_{2j_1,0} + 2\Phi_{02}v_{0,2j_2} + \Phi_{22}v_{2j_1,2j_2}) \\
\langle f_{11}^2, f_{11}\rangle &= 0.
\end{aligned}
$$

Next we substitute (57) into (56) and obtain the following.

$$
\begin{aligned}
\langle g_1, f_{11}\rangle = \frac{L\pi^2}{16}\Big[&4(\phi_2 + \phi_3 v_{0,0})\Phi_{00} + 2(\phi_2 + \phi_3 v_{2j_1,0})\Phi_{20} \\
&+ 2(\phi_2 + \phi_3 v_{0,2j_2})\Phi_{02} + (\phi_2 + \phi_3 v_{2j_1,2j_2})\Phi_{22}\Big] x_1
\end{aligned} \tag{58}
$$

Next we solve for the coefficients of the center manifold functions by first evaluating the following inner products.

$$
\begin{aligned}
&\langle G_{21}, f_{00}\rangle = 4\langle G_{21}, f_{22}\rangle = \frac{L\pi^2}{4}\phi_1 x_1^2 \\
&\langle G_{21}, f_{20}\rangle = \langle G_{21}, f_{02}\rangle = \frac{L\pi^2}{8}\phi_1 x_1^2 \\
&\langle f_{11}, f_{11}\rangle = \langle f_{22}, f_{22}\rangle = \frac{L\pi^2}{4} \\
&\langle f_{20}, f_{20}\rangle = \langle f_{02}, f_{02}\rangle = \frac{L\pi^2}{2} \\
&\langle f_{11}^2, f_{11}\rangle = 0
\end{aligned} \tag{59}
$$

then utilising the equation

$$\frac{d\Phi}{dt} = L(\Phi) + G(u)$$

that is,

$$\frac{d}{dt}\begin{bmatrix}\Phi_u\\ \Phi_v\end{bmatrix} = L\begin{bmatrix}\Phi_u\\ \Phi_v\end{bmatrix} + \begin{bmatrix}G_{21}\\ G_{22}\end{bmatrix} \tag{60}$$

Substituting the terms of the center manifold function in turns we have

$$\begin{aligned} f_{20}\begin{pmatrix}u_{2j_1,0}\\ v_{2j_1,0}\end{pmatrix}\frac{d\Phi_{20}}{dt} &= \beta_{2j_1,0}\Phi_{20}\begin{pmatrix}u_{2j_1,0}\\ v_{2j_1,0}\end{pmatrix} f_{20} + P_2\begin{pmatrix}G_{21}\\ G_{22}\end{pmatrix}\\ \frac{d\Phi_{20}}{dt} &= \beta_{2j_1,0}\Phi_{20} + \left(\frac{1-v_{2j_1,0}}{1+v^2_{2j_1,0}}\right)\frac{\langle G_{21}, f_{20}\rangle}{\langle f_{20}, f_{20}\rangle}\\ &= \beta_{2j_1,0}q_{20}x_1^2 + \left(\frac{1-v_{2j_1,0}}{1+v^2_{2j_1,0}}\right)\frac{\langle G_{21}, f_{20}\rangle}{\langle f_{20}, f_{20}\rangle} \end{aligned} \tag{61}$$

$$\begin{aligned} \frac{d\Phi_{20}}{dt} &= \frac{\partial\Phi_{20}}{dt}\cdot\frac{dx_1}{dt}\\ &= 2q_{20}x_1(\beta_{j_1,j_2}x_1 + \ldots) \end{aligned} \tag{62}$$

By comparing (61) and (62) and following similar computations we can write the coefficients as follows

$$\begin{aligned} q_{00} &= \frac{\phi_1}{4\beta_{0,0}}V_{0,0}, & \Phi_{00} &= \frac{\phi_1}{4\beta_{0,0}}V_{0,0}x_1^2\\ q_{20} &= \frac{\phi_1}{4\beta_{2j_1,0}}V_{2j_1,0}, & \Phi_{20} &= \frac{\phi_1}{4\beta_{2j_1,0}}V_{2j_1,0}x_1^2,\\ q_{02} &= \frac{\phi_1}{4\beta_{0,2j_2}}V_{0,2j_2}, & \Phi_{02} &= \frac{\phi_1}{4\beta_{0,2j_2}}V_{0,2j_2}x_1^2,\\ q_{22} &= \frac{\phi_1}{4\beta_{2j_1,2j_2}}V_{2j_1,2j_2}, & \Phi_{22} &= \frac{\phi_1}{4\beta_{2j_1,2j_2}}V_{2j_1,2j_2}x_1^2 \end{aligned} \tag{63}$$

Thus (58) can be simplified to

$$\langle g_1, f_{11}\rangle = \frac{L\pi^2}{64}\Big(4M_{00} + 2M_{20} + 2M_{02} + M_{22}\Big)x_1^3 \tag{64}$$

Where M_{00}, M_{20}, M_{02} and M_{22} are as defined in (34). When we substitute (64) into (53) we obtain (31). This concludes the proof for this case.

5.1.2. *Single roll mode transition.* We consider a single critical mode with roll pattern

$$f_{10} = e_{j_1,0} = \cos\left(\frac{j_1 x}{L}\right), \quad j_1 \in \mathbb{N}$$

$$\begin{pmatrix}u\\ v\end{pmatrix} = x_1\begin{pmatrix}u_{j_1,0}\\ v_{j_1,0}\end{pmatrix} f_{10} + \begin{pmatrix}\Phi_u\\ \Phi_v\end{pmatrix} \tag{65}$$

$$\begin{aligned} \begin{pmatrix}\Phi_u\\ \Phi_v\end{pmatrix} = \Phi_{00}\begin{pmatrix}u_{0,0}\\ v_{0,0}\end{pmatrix} f_{00} + \Phi_{20}\begin{pmatrix}u_{2j_1,0}\\ v_{2j_1,0}\end{pmatrix} f_{20}\\ + \Phi_{02}\begin{pmatrix}u_{0,2j_2}\\ v_{0,2j_2}\end{pmatrix} f_{02} + \Phi_{11}\begin{pmatrix}u_{j_1,j_2}\\ v_{j_1,j_2}\end{pmatrix} f_{11} \end{aligned} \tag{66}$$

$$\Phi_{00} = m_{00}x_1^2$$
$$\Phi_{20} = m_{20}x_1^2$$
$$\Phi_{02} = m_{02}x_1^2$$
$$\Phi_{11} = m_{22}x_1^2$$

By substituting the center part of the solution (65) into (12) we obtain the following amplitude equations.

$$\frac{dx_1}{dt} = \beta_{j_1,0}x_1 + c\frac{\langle g_1, f_{10}\rangle}{\langle f_{10}, f_{10}\rangle} \tag{67}$$

Following similar process as in the single rectangular mode transition, we cans show that in this case

$$\begin{aligned}
g_1 &= \phi_1 x_1^2 f_{10}^2 + \phi_2 x_1 f_{10}\Phi_u + \phi_3 x_1 f_{10}\Phi_v \\
\langle g_1, f_{10}\rangle &= \phi_1 x_1^2\langle f_{10}^2, f_{10}\rangle + \phi_2 x_1\langle f_{10}\Phi_u, f_{10}\rangle + \phi_3 x_1\langle f_{10}\Phi_v, f_{10}\rangle \\
\langle g_1, f_{10}\rangle &= \frac{L\pi^2}{4}\left[(\phi_2 + \phi_3 v_{2j_1,0})\Phi_{20} + (\phi_2 + \phi_3 v_{0,0})\Phi_{00}\right]x_1 \\
&= \frac{L\pi^2}{4}\left(M_{00} + 1/2M_{20}\right)x_1^3, \\
\langle f_{10}, f_{10}\rangle &= \frac{L\pi^2}{2}, \quad \langle f_{10}^2, f_{10}\rangle = 0, \quad \langle f_{00}, f_{00}\rangle = L\pi^2.
\end{aligned} \tag{68}$$

The coefficients of the center manifold function are computed in a similar fashion as in the single rectangular mode transition.

$$\begin{aligned}
m_{00} &= \frac{\phi_1}{2\beta_{00}}V_{00}, & \Phi_{00} &= \frac{\phi_1}{2\beta_{00}}V_{00}x_1^2, \\
m_{20} &= \frac{\phi_1}{4\beta_{2j_1,0}}V_{2j_1,0}, & \Phi_{20} &= \frac{\phi_1}{4\beta_{2j_1,0}}V_{2j_1,0}x_1^2, \\
m_{02} &= m_{22} = 0.
\end{aligned} \tag{69}$$

Substituting the results in (68) into (67), we obtain the results in (39). This concludes the proof.

5.1.3. *Transitions from double roll mode.* In this case, $r = 2$ and the critical modes are

$$f_{10} = e_{j_1,0} = \cos\left(\frac{j_1 x}{L}\right), \quad f_{01} = e_{0,j_2} = \cos j_2 y, \quad j_1, j_2 \in \mathbb{N}$$

$$\begin{pmatrix} u \\ v \end{pmatrix} = x_1(t)\begin{pmatrix} u_{j_1,0} \\ v_{j_1,0} \end{pmatrix} f_{10} + x_2(t)\begin{pmatrix} u_{0,j_2} \\ v_{0,j_2} \end{pmatrix} f_{01} + \begin{pmatrix} \Phi_u \\ \Phi_v \end{pmatrix} \tag{70}$$

$$\begin{pmatrix} \Phi_u \\ \Phi_v \end{pmatrix} = \Phi_{00}\begin{pmatrix} u_{0,0} \\ v_{0,0} \end{pmatrix} f_{00} + \Phi_{20}\begin{pmatrix} u_{2j_1,0} \\ v_{2j_1,0} \end{pmatrix} f_{20} + \Phi_{02}\begin{pmatrix} u_{0,2j_2} \\ v_{0,2j_2} \end{pmatrix} f_{02} + \Phi_{11}\begin{pmatrix} u_{j_1,j_2} \\ v_{j_1,j_2} \end{pmatrix} f_{11}$$

$$\Phi_{20}(x_1, x_2) = a_{11}x_1^2 + a_{12}x_1x_2 + a_{22}x_2^2$$
$$\Phi_{02}(x_1, x_2) = b_{11}x_1^2 + b_{12}x_1x_2 + b_{22}x_2^2$$
$$\Phi_{11}(x_1, x_2) = c_{11}x_1^2 + c_{12}x_1x_2 + c_{22}x_2^2$$
$$\Phi_{00}(x_1, x_2) = d_{11}x_1^2 + d_{12}x_1x_2 + d_{22}x_2^2$$

By substituting the center part of the solution into (12) we obtain the following amplitude equations.

$$\begin{aligned} \frac{dx_1}{dt} &= \beta_{j_1,0}x_1 + c\frac{\langle g_1, f_{10}\rangle}{\langle f_{10}, f_{10}\rangle} \\ \frac{dx_2}{dt} &= \beta_{0,j_2}x_2 + c\frac{\langle g_1, f_{01}\rangle}{\langle f_{01}, f_{01}\rangle} \end{aligned} \tag{71}$$

where c is as defined in (33) whereas in this case, $g_1(u,v)$ is defined us

(72)
$$g_1(u,v) = \left(x_1^2 f_{10}^2 + 2x_1x_2f_{10}f_{01} + x_2 f_{01}^2\right)\phi_1 + (x_1f_{10} + x_2f_{01})\left(\phi_2\Phi_u + \phi_3\Phi_v\right)$$

In this case the quadratic part of $g_1(u,v)$ is given by

$$G_{21} = \left(x_1^2 f_{10}^2 + 2x_1x_2f_{10}f_{01} + x_2^2 f_{01}^2\right)\phi_1$$

.

Now we evaluate $\langle g_1, f_{10}\rangle$ and $\langle g_1, f_{01}\rangle$ as follows.

$$\begin{aligned} \langle g_1, f_{10}\rangle &= \phi_1\rho_1 + \phi_2\rho_2 + \phi_3\rho_3 \\ \rho_1 &= \langle\left(x_1^2 f_{10}^2 + 2x_1x_2f_{10}f_{01} + x_2^2 f_{01}^2\right), f_{10}\rangle \\ \rho_2 &= \langle(x_1f_{10} + x_2f_{01})\Phi_u, f_{10}\rangle \\ \rho_3 &= \langle(x_1f_{10} + x_2f_{01})\Phi_v, f_{10}\rangle \end{aligned} \tag{73}$$

$$\begin{aligned} \langle g_1, f_{01}\rangle &= \phi_1\tilde{\rho_1} + \phi_2\tilde{\rho_2} + \phi_3\tilde{\rho_3} \\ \tilde{\rho_1} &= \langle\left(x_1^2 f_{10}^2 + 2x_1x_2f_{10}f_{01} + x_2^2 f_{01}^2\right), f_{01}\rangle \\ \tilde{\rho_2} &= \langle(x_1f_{10} + x_2f_{01})\Phi_u, f_{01}\rangle \\ \tilde{\rho_3} &= \langle(x_1f_{10} + x_2f_{01})\Phi_v, f_{01}\rangle \end{aligned} \tag{74}$$

Hence (73) and (74) evaluate to

$$\begin{aligned} \langle g_1, f_{10}\rangle = \frac{L\pi^2}{4}\big[&2(\phi_2 + \phi_3\nu_{00})\Phi_{00}x_1 + (\phi_2 + \phi_3\nu_{2j_1,0})\Phi_{20}x_1 \\ &+ (\phi_2 + \phi_3\nu_{j_1,j_2})\Phi_{11}x_2\big] \\ \langle g_1, f_{01}\rangle = \frac{L\pi^2}{4}\big[&2(\phi_2 + \phi_3\nu_{00})\Phi_{00}x_2 + (\phi_2 + \phi_3\nu_{0,2j_2})\Phi_{02}x_2 \\ &+ (\phi_2 + \phi_3\nu_{j_1,j_2})\Phi_{11}x_1\big] \end{aligned} \tag{75}$$

$$\begin{aligned} \langle G_{21}, f_{20}\rangle &= \tfrac{L\pi^2}{4}\phi_1x_1^2, \quad \langle f_{20}, f_{20}\rangle = \tfrac{L\pi^2}{2} \\ \langle G_{21}, f_{02}\rangle &= \tfrac{L\pi^2}{4}\phi_1x_2^2, \quad \langle f_{02}, f_{02}\rangle = \tfrac{L\pi^2}{2} \\ \langle G_{21}, f_{11}\rangle &= \tfrac{L\pi^2}{2}\phi_1x_1x_2, \quad \langle f_{11}, f_{11}\rangle = \tfrac{L\pi^2}{4} \\ \langle G_{21}, f_{00}\rangle &= \tfrac{L\pi^2}{4}\phi_1(x_1^2 + x_2^2), \quad \langle f_{00}, f_{00}\rangle = L\pi^2 \end{aligned}$$

Now we look for the coefficients of the terms in the center manifold function. We substitute each of the terms of center manifold part of our solution to (12) and take the inner product with respect to respective eigenfunctions as in the previous cases, we obtain the following equations.

$$
\begin{aligned}
\frac{d\Phi_{20}(x_1,x_2)}{dt} &= \beta_{2j_1,0}\Phi_{20} + \left(\frac{1-\nu_{20}}{1+\nu_{20}^2}\right)\frac{\langle G_{21}, f_{20}\rangle}{\langle f_{20}, f_{20}\rangle} \\
\frac{d\Phi_{02}(x_1,x_2)}{dt} &= \beta_{0,2j_2}\Phi_{02} + \left(\frac{1-\nu_{02}}{1+\nu_{02}^2}\right)\frac{\langle G_{21}, f_{02}\rangle}{\langle f_{02}, f_{02}\rangle} \\
\frac{d\Phi_{11}(x_1,x_2)}{dt} &= \beta_{j_1,j_2}\Phi_{11} + \left(\frac{1-\nu_{11}}{1+\nu_{11}^2}\right)\frac{\langle G_{21}, f_{11}\rangle}{\langle f_{11}, f_{11}\rangle}
\end{aligned}
\tag{76}
$$

Equation (76) can also be written alternatively as

$$
\begin{aligned}
\frac{d\Phi_{00}}{dt} &= \frac{\partial\Phi_{00}}{\partial x_1}.\frac{dx_1}{dt} + \frac{\partial\Phi_{00}}{\partial x_2}.\frac{dx_2}{dt} \\
\frac{d\Phi_{20}}{dt} &= \frac{\partial\Phi_{20}}{\partial x_1}.\frac{dx_1}{dt} + \frac{\partial\Phi_{20}}{\partial x_2}.\frac{dx_2}{dt} \\
\frac{d\Phi_{02}}{dt} &= \frac{\partial\Phi_{02}}{\partial x_1}.\frac{x_1}{dt} + \frac{\partial\Phi_{02}}{\partial x_2}.\frac{dx_2}{dt} \\
\frac{d\Phi_{11}}{dt} &= \frac{\partial\Phi_{11}}{\partial x_1}.\frac{dx_1}{dt} + \frac{\partial\Phi_{11}}{\partial x_2}.\frac{dx_2}{dt}
\end{aligned}
\tag{77}
$$

By comparing (76) and (77) we obtain the following results for the coefficients.

$$
\begin{aligned}
& d_{11} = d_{11} = \frac{\phi_1}{2\beta_{0,0}}V_{0,0}, \quad d_{12} = 0 \\
& a_{11} = \frac{\phi_1}{2\beta_{2j_1,0}}V_{2j_1,0}, \quad a_{12} = a_{22} = 0 \\
& b_{22} = \frac{\phi_1}{2\beta_{0,2j_2}}V_{0,2j_2}, \quad b_{11} = b_{12} = 0 \\
& c_{12} = \frac{2\phi_1}{\beta_{j_1,j_2}}V_{j_1,j_2}, \quad c_{11} = c_{22} = 0
\end{aligned}
\tag{78}
$$

Substituting (78) into (75), We obtain

$$
\begin{aligned}
\langle g_1, f_{10}\rangle &= \frac{L\pi^2}{4}\left[(M_{00} + 1/2M_{20})x_1^3 + (M_{00} + 2M_{11})x_1x_2^2\right] \\
\langle g_1, f_{01}\rangle &= \frac{L\pi^2}{4}\left[(M_{00} + 2M_{11})x_1^2x_2 + (M_{00} + 1/2M_{02})x_2^3\right]
\end{aligned}
\tag{79}
$$

By putting (79) into (71) simplifies to (41).

The steady states for (41) are as follows,

$$
\begin{aligned}
& P_0 = (0,0) \\
& P_1^{\pm} \equiv \left(0, \pm\sqrt{\frac{-\beta_{j_1,0}}{D_2}}\right), \quad \beta_{j_1,0}D_2 < 0 \\
& P_2^{\pm} \equiv \left(\pm\sqrt{\frac{-\beta_{j_1,0}}{D_2}}, 0\right), \quad \beta_{10}D_2 < 0 \\
& M^{\pm} \equiv \left(\pm\sqrt{\frac{-\beta_{j_1 0}}{D_1+D_2}}, \pm\sqrt{\frac{-\beta_{j_1,0}}{D_1+D_2}}\right), \quad \beta_{j_1,0}(D_1+D_2) < 0
\end{aligned}
\tag{80}
$$

$P_1^{\pm}$ and $P_2^{\pm}$ are steady states for the pure modes while $M^{\pm}$ represents the steady states of the mixed modes. We define the Jacobian,

$$
J(x_1,x_2) = \begin{bmatrix} \beta_{j_1,0} + D_1x_2^2 + 3D_2x_1^2 & 2D_1x_1x_2 \\ 2D_1x_1x_2 & \beta_{j_1,0} + D_1x_1^2 + 3D_2x_2^2 \end{bmatrix}
\tag{81}
$$

$$J(P_0) = \begin{bmatrix} \beta_{j_1,0} & 0 \\ 0 & \beta_{j_1,0} \end{bmatrix} \tag{82}$$

P_0 is unstable if $\lambda_0 = \beta_{j_1,0} > 0$ and stable if $\lambda_0 = \beta_{j_1,0} < 0$.

$$J(P_1^{\pm}) = \begin{bmatrix} \frac{(D_2-D_1)}{D_2}\beta_{j_1,0} & 0 \\ 0 & -2\beta_{j_1,0} \end{bmatrix} \tag{83}$$

From (80), $\lambda_1^{P_1} = \frac{1}{D_2}(D_2 - D_1)\beta_{j_1,0}$ and $\lambda_2^{P_1} = -2\beta_{j_1,0}$ and also from (81), $\lambda_2^{P_1} = -2\beta_{j_1,0}$ and $\lambda_1^{P_2} = \frac{1}{D_2}(D_2 - D_1)\beta_{j_1,0}$. Therefore P_1, P_2 are stable when $\beta_{j_1,0} > 0$ and $D_1 < D_2 < 0$.

$$J(P_2^{\pm}) = \begin{bmatrix} -2\beta_{j_1,0} & 0 \\ 0 & \frac{(D_2-D_1)}{D_2}\beta_{j_1,0} \end{bmatrix} \tag{84}$$

$$J(M^{\pm}) = \begin{bmatrix} \frac{-2D_2}{D_1+D_2}\beta_{j_1,0} & \frac{2D_1}{D_1+D_2}\beta_{j_1,0} \\ \frac{2D_1}{D_1+D_2}\beta_{j_1,0} & \frac{-2D_2}{D_1+D_2}\beta_{j_1,0} \end{bmatrix} \tag{85}$$

To analyze the stability of $M^{\pm}$ we find the trace and the determinant as follows

$$\tau = \frac{-4D_2}{D_1+D_2}\beta_{j_1,0} \tag{86}$$

$$\Delta = \frac{4(D_2-D_1)\beta_{j_1,0}^2}{(D_1+D_2)} \tag{87}$$

Thus $M^{\pm}$ is stable when $\tau < 0$ and $\Delta > 0$ and unstable otherwise. From Theorem 3 and from the trace and determinant of the jacobian matrix of the truncated vector field, we can draw the following conclusions.

(1) The structure of the attractor depends on the signs of the parameters D_1, D_2 and on the sum $D_1 + D_2$. The signs of D_1, D_2 can either be negative or positive.
(2) The trace, τ is negative when $D_1 + D_2 < 0$ and positive when $D_1 + D_2 > 0$ since for the existence of the steady states for the pure modes, we require $\beta_{10}D_2$ to be negative always.
(3) The determinant, Δ is positive when both $D_2 - D_1$ and $D_2 + D_1$ have the same sign and negative when their signs alternates.
(4) Only cases (i) and (ii) under Theorem 3 are possible because each of cases (iii), (iv) and (v) lead to four steady states on the attractor which are all unstable.

5.1.4. *Transitions from a roll mode and a rectangular mode.* In this case $r = 2$ and the critical modes are

$$f_{11} = e_{j_1,j_2} = \cos\left(\frac{j_1 x}{L}\right)\cos(j_2 y), \quad f_{20} = e_{2j_1 0} = \cos\left(\frac{2j_1 x}{L}\right) \quad j_1, j_2 \in \mathbb{N}$$

$$\begin{pmatrix} u \\ v \end{pmatrix} = x_1(t)\begin{pmatrix} u_{j_1,j_2} \\ v_{j_1,j_2} \end{pmatrix} f_{11} + x_2(t)\begin{pmatrix} u_{2j_1,0} \\ v_{2j_1,0} \end{pmatrix} f_{20} + \begin{pmatrix} \Phi_u \\ \Phi_v \end{pmatrix} \tag{88}$$

$$\begin{aligned}\begin{pmatrix}\Phi_u\\ \Phi_v\end{pmatrix} = \Phi_{00}\begin{pmatrix}u_{0,0}\\ v_{0,0}\end{pmatrix} f_{00} + \Phi_{40}\begin{pmatrix}u_{4j_1,0}\\ v_{4j_1,0}\end{pmatrix} f_{40} + \Phi_{31}\begin{pmatrix}u_{3j_1,j_2}\\ v_{3j_1,j_2}\end{pmatrix} f_{3j_1,j_2}\\ +\Phi_{22}\begin{pmatrix}u_{2j_1,2j_2}\\ v_{2j_1,2j_2}\end{pmatrix} f_{22}\end{aligned} \tag{89}$$

$$\begin{aligned}\Phi_{00}(x_1,x_2) &= q_{11}x_1^2 + q_{12}x_1x_2 + q_{22}x_2^2\\ \Phi_{40}(x_1,x_2) &= h_{11}x_1^2 + h_{12}x_1x_2 + h_{22}x_2^2\\ \Phi_{31}(x_1,x_2) &= m_{11}x_1^2 + m_{12}x_1x_2 + m_{22}x_2^2\\ \Phi_{22}(x_1,x_2) &= n_{11}x_1^2 + n_{12}x_1x_2 + n_{22}x_2^2\end{aligned}$$

By substituting the center part of the solution in (12) we obtain the following amplitude equations as in the previous cases,

$$\begin{aligned}\frac{dx_1}{dt} &= \beta x_1 + c\frac{\langle g_1, f_{11}\rangle}{\langle f_{11}, f_{11}\rangle}\\ \frac{dx_2}{dt} &= \beta x_2 + c\frac{\langle g_1, f_{20}\rangle}{\langle f_{20}, f_{20}\rangle}\end{aligned} \tag{90}$$

such that at the critical crossing, we have let

$$\beta_{2j_1,0} = \beta_{j_1,j_2} = \beta$$

Also, c is as defined in (33) and in this case $g_1(u,v)$ is given below

$$\begin{aligned}g_1 =&\phi_1(x_1^2f_{11}^2 + 2x_1x_2f_{20}f_{11} + x_2^2f_{20}^2) + \phi_2(x_1f_{11} + x_2f_{20})\Phi_u +\\ &\phi_3(x_1f_{11} + x_2f_{20})\Phi_v\end{aligned} \tag{91}$$

In this case the quadratic part of g_1 is given by

$$G_{21} = \phi_1(x_1^2f_{11}^2 + 2x_1x_2f_{20}f_{11} + x_2^2f_{20}^2) \tag{92}$$

Now we evaluate $\langle g_1, f_{20}\rangle$ and $\langle g_1, f_{11}\rangle$ as follows.

$$\begin{aligned}\langle g_1, f_{11}\rangle = \phi_1\rho_1 + \phi_2\rho_2 + \phi_3\rho_3&\\ \rho_1 &= \langle(x_1^2f_{11}^2 + 2x_1x_2f_{20}f_{11} + x_2^2f_{20}^2), f_{11}\rangle\\ \rho_2 &= \langle(x_1f_{11} + x_2f_{20})\Phi_u, f_{11}\rangle\\ \rho_3 &= \langle(x_1f_{11} + x_2f_{20})\Phi_v, f_{11}\rangle\end{aligned} \tag{93}$$

Therefore

$$\begin{aligned}\rho_1 &= \frac{L\pi^2}{4}x_1x_2\\ \rho_2 &= \frac{L\pi^2}{16}(4\Phi_{00}x_1 + \Phi_{22}x_1 + 2\Phi_{31}x_2)\\ \rho_3 &= \frac{L\pi^2}{16}(4\Phi_{00}v_{00}x_1 + \Phi_{22}v_{2j_1,2j_2}x_1 + 2\Phi_{31}x_2)\end{aligned} \tag{94}$$

Similarly,

$$\begin{aligned}\langle g_1, f_{20}\rangle = \phi_1\tilde{\rho_1} + \phi_2\tilde{\rho_2} + \phi_3\tilde{\rho_3}&\\ \tilde{\rho_1} &= \langle(x_1^2f_{11}^2 + 2x_1x_2f_{20}f_{11} + x_2^2f_{20}^2), f_{20}\rangle\\ \tilde{\rho_2} &= \langle(x_1f_{11} + x_2f_{20})\Phi_u, f_{20}\rangle\\ \tilde{\rho_3} &= \langle(x_1f_{11} + x_2f_{20})\Phi_v, f_{20}\rangle\end{aligned} \tag{95}$$

Therefore,

$$\tag{96}\begin{aligned}\tilde{\rho_1} &= \frac{L\pi^2}{8}x_1^2\\ \tilde{\rho_2} &= \frac{L\pi^2}{8}\left(4\Phi_{00}x_2 + \Phi_{31}x_1 + 2\Phi_{40}x_2\right)\\ \tilde{\rho_3} &= \frac{L\pi^2}{8}\left(4\Phi_{00}\nu_{00}x_2 + \Phi_{31}\nu_{3j_1,j_2}x_1 + 2\Phi_{40}\nu_{4j_1,0}x_2\right)\end{aligned}$$

$$\langle f_{20}, f_{20}\rangle = \frac{L\pi^2}{2}, \qquad \langle f_{11}, f_{11}\rangle = \frac{L\pi^2}{4}$$

Finally,

$$\tag{97}\begin{aligned}\langle g_1, f_{11}\rangle &= \frac{L\pi^2}{16}\left[4\phi_1 x_1 x_2 + 2\left(M_{00}+M_{31}\right)x_1x_2^2 + \left(\frac{M_{22}}{4}+M_{00}\right)x_1^3\right]\\ \langle g_1, f_{20}\rangle &= \frac{L\pi^2}{8}\left[\phi_1 x_1^2 + \left(M_{00}+M_{31}\right)x_1^2x_2 + (2M_{00}+M_{40})x_2^3\right]\end{aligned}$$

Such that

$$\tag{98}\begin{aligned}\Phi_{40} &= \frac{V_{4j_1,0}}{2\beta_{4j_1,0}}x_2^2, \qquad & \Phi_{31} &= \frac{V_{3j_1,j_2}}{\beta_{3j_1,j_2}}x_1x_2\\ \Phi_{22} &= \frac{V_{2j_1,2j_2}}{4\beta_{2j_1,j_2}}x_1^2, \qquad & \Phi_{00} &= \frac{V_{0,0}}{4\beta_{0,0}}(x_1^2+2x_2^2)\end{aligned}$$

Substituting (97) into (90), we obtain the reduced (amplitude) equation (45). We refer the interested reader to [17] for further detailed analysis on this case.

References

[1] Y. Choi, T. Ha, J. Han, S. Kim, D. S. Lee, Turing instability and dynamic phase transition for the Brusselator model with multiple critical eigenvalues, Discrete & Continuous Dynamical Systems 41 (9) (2021) 4255. doi:10.3934/dcds.2021035.

[2] T. Ma, S. Wang, Phase Transitions for the Brusselator Model, Journal of Mathematical Physics 52 (3) (2011) 033501. arXiv:1008.1374, doi:10.1063/1.3559120.

[3] T. Ma, S. Wang, Phase Transition Dynamics, Springer International Publishing, Cham, 2019. doi:10.1007/978-3-030-29260-7.

[4] T. Ma, S. Wang, Dynamic transition theory for thermohaline circulation, Physica D: Nonlinear Phenomena 239 (3-4) (2010) 167–189. doi:DOI:10.1016/j.physd.2009.10.014.

[5] T. Ma, S. Wang, Dynamic transition and pattern formation for chemotactic systems, Discrete & Continuous Dynamical Systems - B 19 (9) (2014) 2809. doi:10.3934/dcdsb.2014.19.2809.

[6] L. Jia, L. Li, Stability and dynamic transition of vegetation model for flat arid terrains, Discrete & Continuous Dynamical Systems - B (2021). doi:10.3934/dcdsb.2021189.

[7] A. Sekisaka, H. Yamamoto, Instability in the nebula model of compressive viscous gases, Physica D: Nonlinear Phenomena 403 (2020) 132290. doi:10.1016/j.physd.2019.132290.

[8] Z. Pan, C. Kieu, Q. Wang, Hopf bifurcations and transitions of two-dimensional quasi-geostrophic flows, Communications on Pure & Applied Analysis 0 (0) (2021) 0. doi:10.3934/cpaa.2021025.

[9] C. Lu, Y. Mao, Q. Wang, D. Yan, Hopf bifurcation and transition of three-dimensional wind-driven ocean circulation problem, Journal of Differential Equations 267 (4) (2019) 2560–2593. doi:10.1016/j.jde.2019.03.021.

[10] J. C. Tzou, B. J. Matkowsky, V. A. Volpert, Interaction of Turing and Hopf modes in the superdiffusive Brusselator model, Applied mathematics letters 22 (9) (2009) 1432–1437.

[11] B. Guo, Y. Han, Attractor and spatial chaos for the Brusselator in RN, Nonlinear Analysis: Theory, Methods & Applications 70 (11) (2009) 3917–3931.

[12] I. Prigogine, R. Lefever, Symmetry breaking instabilities in dissipative systems. II, The Journal of Chemical Physics 48 (4) (1968) 1695–1700.

[13] P. C. Rech, Multistability in a Periodically Forced Brusselator, Brazilian Journal of Physics 51 (1) (2021) 144–147. doi:10.1007/s13538-020-00806-2.

[14] D. S. Seara, B. B. Machta, M. P. Murrell, Irreversibility in dynamical phases and transitions, Nature Communications 12 (1) (2021) 392. doi:10.1038/s41467-020-20281-2.

[15] J. Llibre, C. Valls, Global qualitative dynamics of the Brusselator system, Mathematics and Computers in Simulation 170 (2020) 107–114.

[16] J. D. Murray, Mathematical Biology II: Spatial Models and Biomedical Applications, 3rd Edition, Interdisciplinary Applied Mathematics, Mathematical Biology, Springer-Verlag, New York, 2003. doi:10.1007/b98869.

[17] T. Şengül, Dynamical transition theory of hexagonal pattern formations, Communications in Nonlinear Science and Numerical Simulation 91 (2020) 105455. doi:10.1016/j.cnsns.2020.105455.

[18] T. Sengul, J. Shen, S. Wang, Pattern formations of 2D Rayleigh-Bénard convection with no-slip boundary conditions for the velocity at the critical length scales, Mathematical Methods in the Applied Sciences 38 (17) (2015) 3792–3806. doi:10.1002/mma.3317.

(Muntari) Department of Mathematics, Marmara University, 34722 Istanbul, Turkey
Email address: umarfaruk19@marun.tr

(Şengül) Department of Mathematics, Marmara University, 34722 Istanbul, Turkey
Email address: taylan.sengul@marmara.edu.tr